EFFECT OF ORGANOMODIFIED NANOCLAY IN POLY (3-HYDROXYBUTYRATE) (PHB)-, EPOXIDIZED NATURAL RUBBER (ENR-50) AND PHB/ENR-50 BLEND NANOCOMPOSITES

By

ALI SALEHABADI

Thesis submitted in fulfillment of the requirements for the degree of

Doctor of Philosophy

September 2014

ACKNOWLEDGEMENTS

I sincerely thank Prof. Mohamad Abu Bakar for his critical guidance through the ups and downs of this journey. I sincerely thank him for serving as chair for my dissertation committee. His untiring support and encouragement throughout last three years has made the path very clear. I thank him for his time during long discussion-hours and dedicated just to clear the knots in this research. His ideas always gave a new dimension to the research, and proposed many different aisles of solution. He taught us the meaning of doing the right thing, performed in a right manner at the right time to achieve maximum output. I extend my heartfelt thanks to Dr. Noor Hana Hanif Abu Bakar for her informative information and her ability to cover obscure and abstract concepts in no time. Her vast knowledge and experience, which she also shared during my paper publishing, were of great value. Amid her busy schedule she always had time to say a quick hello with a smile and heeded to what I had to say. I sincerely thank all my great friends in our group, Rosniza Hamzah, Noorul Ain, Siew Yean, Chew Ker Yin, Atoosa Haghighizadeh for their tacit support, thoughtful concern, and unselfish care during hard times. I must acknowledge the staffs of the School of Chemical Sciences at Univeristi Sains Malaysia, Mr. Ali, Mr. Baharuddin, Mr.Ong, Mrs. Azila Ani and Mr. Ashamuddin at School of Mechanical Engineering and many more for their support. Many thank to the Universiti Sains Malaysia for financial support in the form of the USM-RU-PRGS: 1001/PKIMIA/844062 over RM 19000.

Again, I sincerely thank to all my dear friends and family, Willawan Jansri, Hossein Azarian, Mehrshad Parvin Hosseini, Pooneh, Mona Khosravi, Soheila Faraji, Niloofar Fallah, and many more for his ever-smiling approach and

encouragement throughout and an especial acknowledge to my old friend Reza Alvani for his encouragement and mental support. They absolutely were a source of strength in me.

Finally, I owe my deepest and heartfelt gratitude to my great teachers during my life; my parents, my only brother, Reza and his wife, Maryam who stood beside me and supported me full heartedly. Their unmatched sacrifice, unlimited love and affectionate blessing have made me successfully complete the thesis.

"*Humbly, I thank them for all that they are to me*"

Ali.Salehabadi

March 2014

TABLE OF CONTENT

ACKNOWLEDGEMENTS ..... **ii**

TABLE OF CONTENT ..... **iv**

TABLE OF SCHEMES ..... **ix**

LIST OF TABLES ..... **x**

TABLE OF FIGURES ..... **xii**

LIST OF ABBREVIATIONS AND SYMBOLS ..... **xvii**

ABSTRAK ..... **xxi**

ABSTRACT ..... **xxii**

CHAPTER 1- RESEARCH BACKGROUND

1.1 Introduction 1

1.2 Polymer Blends 3

1.3 Hybrids and Composites 5

1.4 Poly (3-hydroxybutyrate) 7

1.5 Epoxidized Natural Rubber (ENR-50) 9

1.6 PHB and ENR-based Immiscible Blends 11

1.7 Clay 14

1.8 Swelling/Expansion of Silicate Layers in Montmorillonite 17

1.9 Organomodified Montmorillonite 19

1.10 Clay-Containing Polymeric Nanocomposites (CPNC) 20

1.10.1 PHB/Clay Nanocomposites 22

1.10.2 ENR/Clay Nanocomposites 25

1.10.3 Clay-Multi-Component Polymer Nano/micro Composites 28

1.11 Problem Statements 30

1.12 Objectives of Research 31

1.13 Scope of Research.....32

1.14 Thesis Layout 33

CHAPTER 2- THEORETICAL BACKGROUND

2.1 Thermal Transitions and Crystallization.....35

2.2 Thermal Degradation 37

2.3 Kissinger Equation.....38

2.4 Nanoindentation.....41

CHAPTER 3- MATERIALS AND METHODS

3.1 Materials.....44

3.2 Purification Procedure 45

3.3 Preparation of Blends and Nanohybrids 45

3.4 Spectroscopic Analysis 46

3.5 Differential Scanning Calorimeter (DSC).....46

3.6 Thermogravimetric (TG) Analysis 47

3.7 Polarized Optical Microscope (POM) 47

3.8 Scanning Electron Microscope (SEM) 48

3.9 X-ray Diffraction Analysis.....48

3.10 Nanoindentator 49

CHAPTER 4- POLY(3-HYDROXYBUTYRATE)- ORGANOMODIFIED MONTMORILLONITE NONOCOMPOSITES

4.1 Introduction 50

4.2 FTIR Spectroscopy 51

4.3 Morphology 56

4.3.1 Polarized Optical Microscopy (POM) 56

4.3.2 Scanning Electron Microscopy (SEM) 60

4.4 Thermal Behavior 62

4.4.1 Differential Scanning Calorimetry (DSC) 62

4.4.2 Thermogravimetry (TG-DTG) 65

4.5 Kinetic of Thermal Degradation 68

4.6 Bulk Structural Study and Clay Interaction 70

4.7 Nanomechanical Properties 72

4.8 Summary 77

CHAPTER 5- EPOXIDIZED NATURAL RUBBER-ORGANOMODIFIED MONTMORILLONITE NANOCOMPOSITES

5.1 Introduction 78

5.2 FTIR Spectroscopy 79

5.3 Morphology 82

5.3.1 Polarized Optical Microscopy (POM) 82

5.3.2 Scanning Electron Microscopy (SEM) 84

5.4 Thermal Behavior 86

5.4.1 Differential Scanning Calorimetry (DSC) 86

5.4.2 Thermogravimetry (TG-DTG) 88

5.5 Kinetic of Thermal Degradation 91

5.6 Bulk Structure and Clay Interaction 92

5.7 Nanomechanical Properties 96

5.8 Summary 99

CHAPTER 6- BINARY IMMISCIBLE POLYMER BLENDS BASED ON PHB AND ENR-50

6.1 Introduction 100

6.2 FTIR Spectroscopy 101

6.3 Surface Analysis and Interphase Study 105

6.3.1 Polarized Optical Microscopy (POM) 105

6.3.2 Scanning Electron Microscopy (SEM) 108

6.4 Thermal Behavior 110

6.4.1 Differential Scanning Calorimetry (DSC) 110

6.4.2 Thermal Decomposition (TG-DTG) 114

6.5 Summary 116

CHAPTER 7- NANOCLAY DISTRIBUTION AND ITS INFLUENCE ON PROPERTY PROFILES OF PHB/ENR-50 BLENDS

7.1 Introduction 118

7.2 FTIR Spectroscopy 119

7.3 Surface Morphology 128

7.3.1 Polarized Optical Microscopy (POM) 128

7.3.2 Scanning Electron Microscopy (SEM) 132

7.4 Thermal Behavior 135

7.4.1 Differential Scanning Calorimetry (DSC) 135

7.4.2 Thermogravimetry (TG-DTG) 140

7.5 Kinetic of Thermal Degradation 147

7.6 Nanoclay Interaction and Bulk Structural Study (XRD) 150

7.7 Nanomechanical Properties 153

7.8 Summary 156

CHAPTER 8- CONCLUSION 158

REFERENCE 163

APPENDICES

LIST OF SCHEMES

Scheme 1.1	Classification of biodegradable polymers	2
Scheme 1.2	Common types of nanocrystalline materials	7
Scheme 1.3	PHB random chain scission	9
Scheme 1.4	In-situ performic acid epoxidation of natural rubber	10
Scheme 1.5	Ring opening reaction of epoxide group of ENR chain under acidic and basic conditions	11
Scheme 1.6	Clay minerals classifications	15
Scheme 1.7	The side view of various clay structures	17
Scheme 1.8	Open structure of montmorillonite	18
Scheme 4.1	Proposed reaction between PHB and MMT	54
Scheme 5.1	Ring opening reaction of ENR-50 via formation of covalent bond	82
Scheme 6.1	Possible reaction in PHB/ENR-50 blends	105
Scheme 7.1	Reaction possibilities of silicate layer/APTES/ODA and PHB/ENR-50 blends with MMT	122

LIST OF TABLES

Table 1.1	Classification of poly-blends	3
Table 4.1	Thermal transitions of PHB and various PHB/MMT nanohybrids	63
Table 4.2	Thermal degradation temperature of PHB, various PHB/MMT nanohybrids and MMT	66
Table 4.3	Kinetic parameters of PHB and its respective PHB/MMT nanohybrids	69
Table 4.4	XRD parameters of PHB, various PHB/MMT nanohybrids and MMT	72
Table 4.5	Nano-mechanical properties of PHB and its respective nanohybrids containing 1, 3 and 5 wt% MMT content	74
Table 5.1	First heating DSC thermal transitions of ENR-50 and its respective nanohybrids and MMT	86
Table 5.2	Thermal degradation data of ENR-50, and various ENR-50/MMT nanohybrids	88
Table 5.3	Kinetic parameters of ENR-50, and its respective nanohybrids containing 1, 3 and 5 wt% MMT	91
Table 5.4	XRD parameters of various ENR-50/MMT nanohybrids and MMT	94
Table 5.5	Nano-mechanical properties of ENR-50 and its respective ENR-50/MMT nanohybrids	96
Table 6.1	Thermal transitions of PHB, various PHB/ENR-50 blends and ENR-50 from 1st and 2nd heating programs	111

Table 6.2	Thermal degradation temperatures of PHB, various PHB/ENR-50 blends and ENR-50	116
Table 7.1	Thermal transition of various PHB/ENR-50 blends containing 1, 3 and 5 wt% MMT from 1st heating program	139
Table 7.2	Thermal transition and thermal decomposition data of PHB/ENR-50 (70/70, 50/50 and 30/70) blends and respective nanohybrids containing 1, 3 and 5 wt% MMT	147
Table 7.3	Kinetic parameters PHB/ENR-50 blend and its respective nanohybrids	148
Table 7.4	XRD parameters of PHB/ENR-50 (50/50) blend containing 1, 3 and 5 wt% MMT and MMT	153
Table 7.5	Nano-mechanical properties of PHB/ENR-50 (50/50) blends containing various wt% MMT content	154

TABLE OF FIGURES

Figure 2.1	Typical loading-hold-unloading sequence	41
Figure 3.1	SEM-EDX of Nanomer® 1.31 PS	44
Figure 4.1	FTIR spectra of PHB and various PHB/MMT nanohybrids and MMT	52
Figure 4.2	Localized FTIR spectra of carbonyl groups of PHB and various PHB/MMT nanohybrids 1, 3 and 5 wt% MMT	55
Figure 4.3	Polaraized Optical Micrographs of neat PHB (a) at room temperature (~25 ºC), (b) at molten state (~174 ºC) and (c) at re-crystallization temperature (~60 ºC)	57
Figure 4.4	Polarized Optical Micrographes of various PHB/MMT nanohybrids containing (a) 1, (b) 3 and (c) 5 wt% MMT	59
Figure 4.5	SEM images of various PHB/MMT nanohybrids containing (a) 1, (b) 3 and (c) 5 wt% MMT	61
Figure 4.6	First heating DSC thermograms of PHB and various PHB/MMT nanohybrids at 20 ºC/min	64
Figure 4.7	Second heating DSC thermograms of PHB and various PHB/MMT nanohybrids at 20 ºC/min.	64
Figure 4.8	(a) TG and (b) DTG curves of PHB, various PHB/MMT nanohybrids and MMT	67
Figure 4.9	Activation energy (E_d) by Kissinger method; (♦) neat PHB, various PHB/MMT nanohybrids containing (■) 1, (▲) 3 and (●) 5 wt% MMT	69

Figure 4.10	XRD patterns of neat PHB, Various PHB/MMT nanohybrids containing 1, 3 and 5 wt% MMT and MMT	71
Figure 4.11	Load-depth curves of PHB and its respective PHB/MMT nanohybrids	73
Figure 4.12	Hardness and Modulus of neat PHB and its nanohybrids with various wt% MMT content	75
Figure 4.13	Ratio of average modulus to hardness (E/H) versus MMT loading for the PHB/MMT nanohybrids containing 0, 1, 3 and 5 wt% MMT	78
Figure 5.1	FTIR spectra of ENR-50, the various ENR-50/MMT nanohybrids containing 1, 3, 5 wt% MMT and MMT	80
Figure 5.2	Localized epoxy rings characteristics bands of ENR-50 and its respective ENR-50/MMT nanohybrids and MMT	81
Figure 5.3	Polarized Optical Micrographs of (a) ENR-50, ENR-50/MMT nanohybrids containing 0, 1, 3 and 5 wt% MMT	83
Figure 5.4	SEM micrographs of various ENR-50/MMT nanohybrids containing (a) 1, (b) 3and (c) 5 wt% MMT	85
Figure 5.5	1^{st} heating DSC thermograms of ENR-50 and various ENR-50/MMT nanohybrids	87
Figure 5.6	(a) TG and (b) DTG curves of ENR-50, various ENR-50/MMT containing 1, 3, 5 wt% MMT and MMT	90
Figure 5.7	Determination of activation energy (E_d) by Kissinger method; (●) ENR-50, ENR containing (▲) 1, (■) 3 and (♦) 5 wt% MMT	92

Figure 5.8	XRD patterns of ENR-50, various ENR-50/MMT nanohybrids containing 1, 3 and 5 wt% MMT and MMT	95
Figure 5.9	Load-displacement curves of various ENR-50/MMT nanohybrids containing 1, 3, 5 wt% MMT	98
Figure 5.10	Hardness and Modulus of ENR-50 and its nanohybrids with various MMT loading	98
Figure 6.1	FTIR spectra of PHB, the various PHB/ENR-50 blends and ENR-50	103
Figure 6.2	Localized spectra of carbonyl bands, epoxy and half epoxy ring of PHB, various PHB/ENR-50 blends and ENR-50	104
Figure 6.3	POM micrographs of various ratios of PHB/ENR-50 comprising (a) 70/30, (b) 50/50 and (c) 30/70	107
Figure 6.4	SEM images of various ratio of PHB/ENR-50 blend comprising 30/70, 50/50 and 70/30	109
Figure 6.5	Proposed schematical morphology of PHB/ENR-50 blend with (a) higher ratio of amorphous domain, (b) equal ratio of each polymers and (c) higher ratio of crystalline polymer, the white color areas represent the PHB and the black color represents the ENR-50 domain	110
Figure 6.6	DSC thermogram of (a) ENR-50, various PHB/ENR-50 blend comprising (b) 30/70, (c) 50/50, (d) 70/30 and (e) PHB from 1st heating program	112
Figure 6.7	DSC thermogram of (a) ENR-50, various PHB/ENR-50 blends comprising (b) 30/70, (c) 50/50, (d) 70/30 and (e) PHB from 2nd heating program	112

Figure 6.8	Glass transition temperature of (a) ENR-50, various PHB/ENR-50 blend comperising (b) 30/70, (c) 50/50, (d) 70/30 and (e) PHB from 2nd heating	113
Figure 6.9	(a) TG and (b) DTG thermograms of PHB, various PHB/ENR-50 blends comprising 70/30, 50/50, 30/70 and ENR-50	115
Figure 7.1	FTIR-ATR spectra of PHB/ENR-50 (30/70) blend and its respective nanohybrids containing 1, 3 and 5 wt% MMT	123
Figure 7.2	FTIR-ATR spectra of PHB/ENR-50 (50/50) blend and respective nanohybrids containing 1, 3 and 5 wt% MMT	124
Figure 7.3	FTIR-ATR spectra of PHB/ENR-50 (70/30) blend and respective nanohybrids containing 1, 3 and 5 wt% MMT	126
Figure 7.4	Localized carbonyl spectra of PHB/ENR-50 (70/30) blend and respective nanohybrids containing 1, 3 and 5 wt% MMT	127
Figure 7.5	POM micrographes of PHB/ENR-50 (30/70) blends containing (a) 1, (b) 3 and (c) 5 wt% MMT	129
Figure 7.6	POM micrographes of PHB/ENR-50 (50/50) blends containing (a) 1, (b) 3 and (c) 5 wt% MMT	130
Figure 7.7	POM micrographes of PHB/ENR-50 (70/30) blends containing (a) 1, (b) 3 and (c) 5 wt% MMT	131
Figure 7.8	SEM micrographs of PHB/ENR-50 (50/50) blends containing (a) 1, (b) 3 and (c) 5 wt% MMT	134
Figure 7.9	DSC thermograms of PHB/ENR-50 (30/70) blends containing 1, 3 and 5 wt% MMT	137
Figure 7.10	DSC thermograms of PHB/ENR-50 (50/50) blends containing	138

1, 3 and 5 wt% MMT

Figure 7.11 DSC thermograms of PHB/ENR-50 (70/30) blends containing 1, 3 and 5 wt% MMT 140

Figure 7.12 (a) TG and (b) DTG thermograms of PHB/ENR-50 (30/70) blends containing 1, 3 and 5 wt% MMT 142

Figure 7.13 (a) TG and (b) DTG thermograms of PHB/ENR-50 (50/50) blends containing 1, 3 and 5 wt% MMT 144

Figure 7.14 (a) TG and (b) DTG thermograms of PHB/ENR-50 (70/30) blends containing 1, 3 and 5 wt% MMT 146

Figure 7.15 Determination of activation energy (E_d) by Kissinger method; (♦) PHB/ENR-50 blend (50/50) containing (■) 1, (▲) 3 and (●) 5 wt% MMT from the (a) 1^{st} maximum and (b) 2^{nd} maximum in DTG profile 149

Figure 7.16 XRD patterns of PHB/ENR-50 (50/50) blend, various PHB/ENR-50 (50/50) blends containing 1, 3 and 5 wt% MMT and MMT 152

Figure 7.17 Load-depth curves of PHB/ENR-50 (50/50) blends containing zero, 1, 3 and 5 wt% MMT 155

Figure 7.18 Hardness and Modulus of PHB/ENR-50 (50/50) blend and its respective nanohybrids with various MMT loading 155

LIST OF ABBREVIAIONS AND SYMBOLS

ϑ_i	Poisson ratio of indenter
ϑ_s	Poisson ratio of sample
Ø	Concentration/Volume fraction
A	Disperse phase parameter
A	Projected contact area/Pre-exponential factor
APTES	Aminopropyltrietoxysilane
ASTM	American society of testing and materials
B	Interaction density parameter
CPNC	Clay containing polymeric nanocomposite
d	Crystallographic spacing
DSC	Diffrential scanning calorimetry
DTG	Derivative thermogravimetry
E_a	Activation energy
E_i	Elastic modulus of indenter
PECH	Polyepichlorohydrin
E_d	Degradation activation energy
EDX	Energy dispersive X-ray
ENR	Epoxidized natural rubber
EPDM	Ethylene propylene dieneter polymer
E_r	Reduce modulus
EVA	Ethylene vinylacetate
FTIR	Fourier transform infrared

H	Hardness
h	Depth
h	displacement
h′	Displacement rate
I	Interaction term
k	Rate constant
MMT	Organomodified montmorillonite
n	Reaction order
NR	Natural rubber
ODA	Octadecylamine
O-sheet	Octahedral sheet
P	Probability/Load/Pressure
PA	Poly(acetylene)
PAA	Poly(acryloamine)
PAN	Poly(acrylonitril)
PANI	Poly(aniline)
PCl	Poly(ε-caprolactone)
PEO	Poly(ethyleneoxide)
PHA	Polyhydroxyalkanoate
PHB	Poly(3-hydroxybutyrate)
PLLA	Polylactic acid
PLSN	Polymer layered silicate nanocomposite
POM	Polarized optical microscopy
Ppy	Polypyrrole
PTH	Polythiophene

PVP	Polyvinylpyrrolidone
R	Gas constant
S	Stiffness
SANS	Small angle neutron scattering
SEM	Scanning electron microscopy
T	Temperature
t	Time
T_c	Crystallization temperature
T_{endset}	Endset temperature
TG	Thermogravimetry
T_g	Glass transition temperature
T_m	Melting temperature
T_{max}	Maximum degradation temperature
T_{onset}	Onset temperature
TO-sheet	Tetrahedral-octahedral sheet
TOT-sheet	Tetrahedral-octahedral-tetrahedral sheet
TPS	Thermoplastic starch
T-sheet	Tetrahedral sheet
V	Volume
wt%	Weight percentage
XRD	X-ray diffraction
α	Fraction
β	Heating rate/Dimensionless correction factor
ΔG	Gibbs(free) energy
ΔH	Enthalpy

ΔS	Entropy
θ	Scattering angle
λ	Wavenumber
φ	Segment fraction

KESAN NANOLEMPUNG TERUBAHSUAI ORGANIK DALAM NANOKOMPOSIT POLI(3-HIDROKSIBUTYRAT) (PHB)-, GETAH ASLI TEREPOKSIDA (ENR-50) DAN ADUNAN PHB/ENR-50

ABSTRAK

Risalah ini mengkaji pengaruh montmorilonit (MMT) diubahsuai dengan organo alkil ammonium terhadap profil ciri poliester terbiodegradasi, PHB, getah asli terubahsuai, ENR-50, dan adunan PHB/ENR-50. Beberapa komposisi hibrid nano telah disediakan dengan penyebaran lapisan MMT nano dalam larutan polimer menggunakan teknik acuan pelarut. Morfologi permukaan dan ciri antara-muka hibrid nano yang berbeza telah dikaji menggunakan mikroskop optik polarisasi (POM) dan imbasan mikroskop elektron (SEM). Morfologi struktur analisis antara-muka menunjukkan suatu pengagihan MMT yang wajar dalam matriks polimer sama ada dengan pengurangan atau pelengkapan pembubaran saiz dan dimensi antara-muka. Kestabilan terma dan peralihan terma dalam sistem telah dicirikan menggunakan masing-masing termogravimetri (TG-DTG) dan perbezaan pengimbasan kalorimetri (DSC). Kestabilan terma sistem yang berbeza berubah dengan penambahan MMT. Lapisan MMT nano mempamerkan sama ada kesan pemangkin atau kesan halangan dalam profil terma hibrid nano. Keupayaan lapisan silikat MMT untuk berinteraksi melalui interkalasi atau pengelupasan dan juga penyusunan semula struktur kristal PHB telah dikaji menggunakan analisis pembelauan X-ray. Pantulan puncak intensiti dan jarak pangkal (d) berubah berdasarkan penambahan MMT. Satah ortorombik kristal PHB (020) dan (110) telah merubah kedudukan dan jarak d apabila kedua-dua ENR-50 dan MMT ditambah. Spektra FTIR menyediakan bukti lanjut yang menyokong kemungkinan reaksi melalui ikatan hidrogen dan pembukaan gelang kumpulan epoksi. Mekanisme tindak balas telah dicadangkan. Plot Kissinger menunjukkan bahawa hibrid nano mempamerkan penurunan tenaga pengaktifan degradasi (E_d). Kajian mekanikal nano sampel ini juga menunjukkan perubahan dalam kekerasan (H) dan modulus elastik (E) apabila berlaku penambahan kandungan MMT dalam sampel.

EFFECT OF ORGANOMODIFIED NANOCLAY IN POLY(3-HYDROXYBUTYRATE) (PHB)-, EPOXIDIZED NATURAL RUBBER (ENR-50) AND PHB/ENR-50 BLEND NANOCOMPOSITES

ABSTRACT

This treatise investigates the influences of alkyl ammonium organomodified montmorillonite (MMT) on the property profiles of biodegradable polyester, PHB, an epoxy modified natural rubber, ENR-50, and their respective PHB/ENR-50 blends. Several compositions of nanohybrids were prepared by dispersion of MMT nanolayers in polymer solution employing solvent casting technique. Surface morphology and interfaces characteristics of different nanohybrids were investigated using polarized optical microscopy (POM) and scanning electron microscopy (SEM). Structural morphology over interfaces analysis indicated a proper distribution of MMT in polymer matrix by either reducing or complete dissolution of interface sizes and dimensions. Thermal stability and thermal transition of the systems were characterized by thermogravimetry (TG-DTG) and differential scanning calorimetry (DSC), respectively. The thermal stability of different systems varied upon addition of MMT. MMT nanolayers exhibited either catalytic or barrier effect in thermal profiles of nanohybrids. The ability of silicate layers of MMT to interact via intercalation or exfoliation and also structural rearrangement of PHB crystals were investigated using X-ray diffraction analysis. The reflected peaks intensities and the basal spacing varied upon addition of MMT. The (020) and (110) orthorhombic crystalline planes of PHB have changed in position and d-spacing upon addition of both ENR-50 and MMT. FTIR spectra provide further evidence that supports the reaction possibilities through the hydrogen bonding and ring opening reaction of epoxy groups. The reaction mechanisms were proposed. The Kissinger plots showed that the nanohybrids exhibited a decrease in degradation activation energy (E_d). The nanomechanical study of these samples indicates changing in hardness (H) and elastic modulus (E) upon increasing MMT content in the sample.

CHAPTER 1

RESEARCH BACKGROUND

1.1 Introduction

Prior to 1917, scientists queried the existence of molecules having molecular weights greater than a few thousand. This limiting view was challenged by Wolfgang Ostwald. He coined the term "the land of neglected dimensions" to describe the range of sizes between molecular and macroscopic within which occur most colloidal particles. Acceptance of the macromolecular hypothesis came about in the 1920's because of the efforts of Staudinger who received the Nobel prize in 1953 [1].

The modern polymer production began with utilization of natural polymers in 1930 like natural rubber and cellulosic products and continued to synthetic polymers. Up to 2008, 200 billion tons per year of wide variety of polymers and plastics are produced, processed and used [2]. The exponential growth of the use of polymeric materials in everyday life has led to the accumulation of huge amounts of non-degradable waste materials across our planet. Environmental concerns caused by disposable of non-degradable plastics have limited the applications.

Initiatives have led to widespread research in biodegradable materials focusing on modifications to make their properties comparable to conventional polymers. According to ASTM D-5488-94d, biodegradable means capable of undergoing decomposition into carbon dioxide, methane, water, inorganic compounds, or biomass in which the predominant mechanism is the enzymatic action of micro-organisms that can be measured by standard tests, over a specific period of time, reflecting available disposal conditions [3]. A vast number of biodegradable

polymers (biopolymers) are synthesized either chemically or bio-synthesized during the growth cycles of organisms. Some microorganisms and enzymes capable of degrading them have been identified. Scheme1.1 [3,4] classifies the biodegradable polymers in four different categories.

Although there is a wide availability of biodegradable polymers, a number of drawbacks have prevented the variety of applications of such polymers. For example, majority of biodegradable polymers are crystalline, exhibit great brittleness and poor impact resistance at room temperature. Moreover, most of them are unstable in molten state and the main problem is of course high production cost of biodegradable polymers. To serve environment and to manufacture the novel biomedical product, modification of biodegradable polymers to everyday use is necessary.

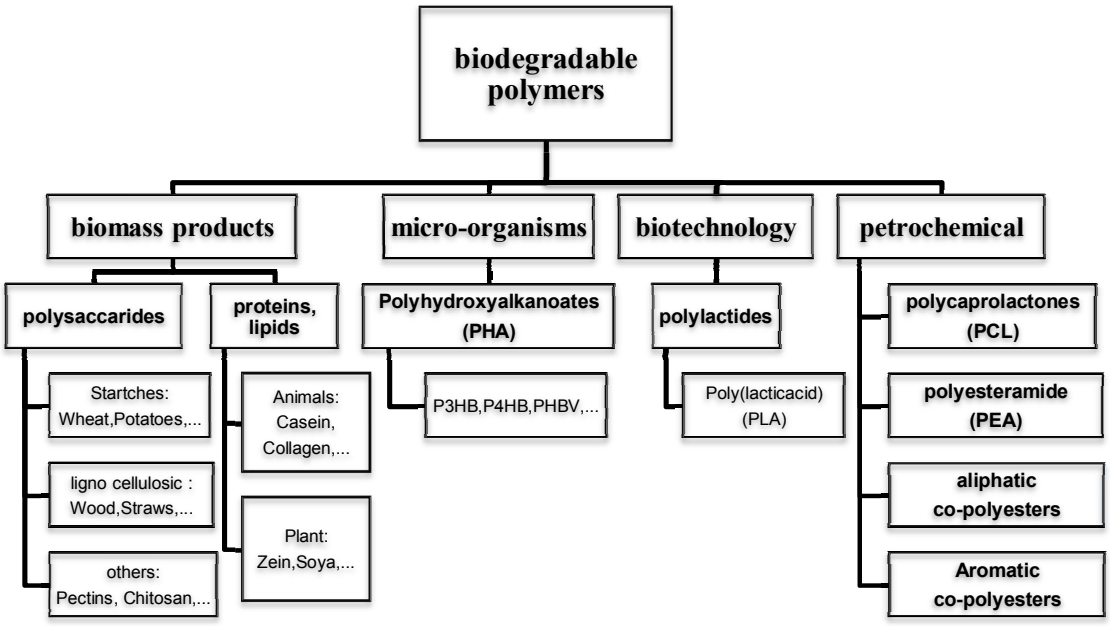

Scheme 1.1: Classification of biodegradable polymers.

1.2 Polymer Blends

In general, mixing together of two or more different polymers or copolymers is known as blending [5]. Compatibility, miscibility and mutual solubility of polymer domains in blend are important factors affecting the properties of blend. Consideration of compatibility between blended polymers is a critical factor in production of new uniform materials having range of properties far different from those of the constituents.

Polymer blends are commonly termed as poly-blends and are processed via several routes namely mechanical polyblend, chemical polyblends, mechano-chemical polyblends, solution casting and latex polyblends. Moreover, various types of poly-blends have been classified (Table 1.1) according to the multitude of polymer alloy compositions. Poly-blends properties are highly dependent on four major factors; extent of phase separation, nature of the phase provided by the matrix material, character of the dispersed phase and interaction between the component polymers.

Table 1.1 Classification of poly-blends [6].

Elastomeric blends [7,8]	Engineering polymer blends [9]
Emulsion blends [10]	Crystalline-crystalline polymer blends [11–14]
Impact modified polymers [15]	Crystalline amorphous polymer blends [9,16,17]
Thermosetting polymer blends [18,19]	Biodegradable polymer blends [3,11,20]
Liquid crystalline polymer blends [21]	Reactive compatibilized blends [22]
Interpenetrating polymer networks [23]	Isomorphic polymer blends [24]
Polyelectrolyte complexes [25]	Polyolefin blends [26]
Recycled polymer blends [22]	Core-shell polymers systems [27,28]
Polymer blend composites [29–31]	Electrically conducting polymer blends [32]
Block copolymer-homopolymer blends[33]	Blends comprising natural polymers [34]

On the basis of as mentioned properties, poly-blends can be classified into miscible, immiscible and partially miscible. In miscible poly-blends, the physical properties obey an arithmetical semi-empirical rule as given by the equation (1.1),

$$P = P_1\emptyset_1 + P_2\emptyset_2 + I\emptyset_1\emptyset_2 \tag{1.1}$$

where P is the probability of interest, $\emptyset_1$ and $\emptyset_2$ are concentrations of matrix and dispersed phase, respectively and I is an interaction term.

For an immiscible poly-blends containing a continuous phase and a dispersed phase, the semiempirical relationship is given by equation (1.2),

$$\frac{P}{P_1} = 1 + AB\emptyset_2 - B\varphi\emptyset_2 \tag{1.2}$$

where ϕ_2 is the concentration of dispersed phase, A is a parameter related to dispersed phase, B is interaction density parameter and φ is segment fraction.

Moreover the thermodynamic of a miscible pair of polymers is obeyed by enthalpy (ΔH_{mix}) and entropy (ΔS_{mix}) of mixing as given by the following equations (1.3),

$$\Delta G_{mix} = \Delta H_{mix} - T\Delta S_{mix} < 0 \tag{1.3}$$

For miscibility to occur, ΔG_{mix} must be smaller than zero. While this is a necessary requirement, it is not a sufficient requirement as the following expression (1.4) must also be satisfied:

$$\left[\frac{\partial^2 \Delta G_{mix}}{\partial \emptyset^2}\right] > 0 \qquad (1.4)$$

where ΔG_{mix},T and $\emptyset$ are free energy of mixing, absolute temperature and volume fraction of a component of poly-blend, respectively. Negative values of equation (1.4) (even though $\Delta G_{mix} < 0$) can yield an area of the phase diagram where the mixture will separate into a phase rich in component 1 and a phase rich in component 2. For low molecular weight materials, increasing the temperature generally lead to increasing miscibility as the $T\Delta S_{mix}$ term increases, thus driving ΔG_{mix} to a more negative value. For higher molecular weight components, the $T\Delta S_{mix}$ term is small and other factors such as non-combinatorial entropy contributions and temperature dependant ΔH_{mix} values can dominate and lead to the reverse behavior, namely, decreasing miscibility with increasing temperature.

In an immiscible blend, the level of interaction is weak and usually gives inferior properties. Reactive blending which improves the miscibility sometimes gives rise to improved properties even better than miscible blends. Glass transition temperature (T_g) of a reactive blend exhibits both negative and positive deviations from linearity, depending on the chain stiffness. Hence, the understanding of polymer-polymer adhesion resulting from both physical or chemical interactions and phase behavior are of primary importance to predict the properties of a poly-blend.

1.3 Hybrids and Composites

The term “hybrid materials” is defined as mixtures of two or more materials with new properties created between each material by formation of chemical bond between organic and inorganic compartments. Nano-ordered composite materials

consisting of organic polymers and inorganic materials have been attracting attention for the purpose of creating high-performance or functional polymeric materials.

The embedding of nanoscopic materials into matrices represents a valid solution to the manipulation and stabilization difficulties. Polymers are interesting embedding phase because of the several characteristics like thermal, electrical and mechanical properties, hydrophobic or hydrophilic nature and so on. Polymer embedding is a convenient way for nanostructured materials, metals or non-metals, stabilization and handling.

In nanomaterials, the shape and interactions between domains determine the properties. This can impart different properties to the final products and also possibility of tailor-making the materials. Mechanical, structural, thermal, electrical, optical and magnetic properties are the most important features of polymer containing nanomaterials.

Due to the shape, several types of nanocrystalline materials can be classified as nanoparticles, nanorods, nanotubes, nanocrystalline solids, granular thin film, homogeneous thin film and multi layers which are schematically illustrated in Scheme 1.2.

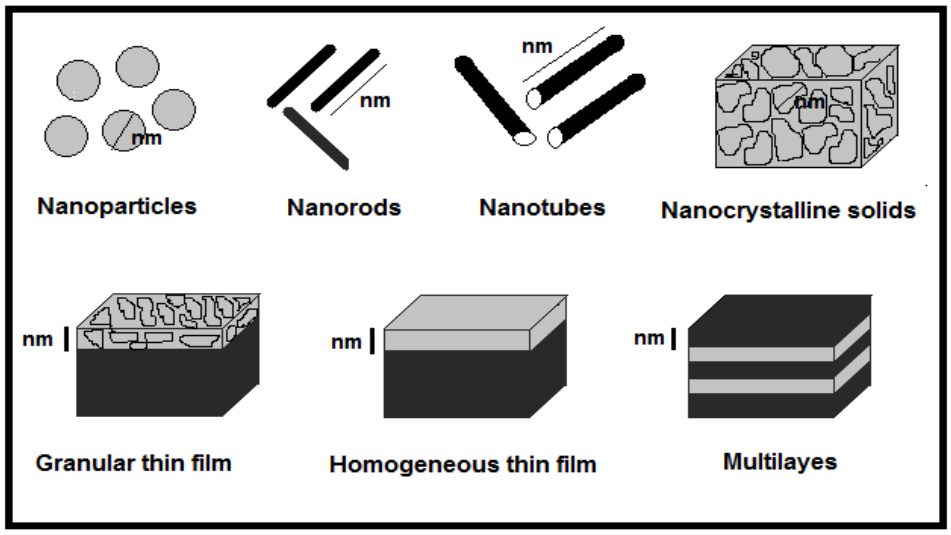

Scheme 1.2: Common types of nanocrystalline materials [35].

1.4 Poly(3-hydroxybutyrate)

The simplest of the family of polyhydroxyalkanoate (PHA) biopolymers is poly(3-hydroxybutyrate). According to ASTM standard D-5488-94d (see Section 1.1), PHB is an aliphatic linear polyester, truly biodegradable and biocompatible material [36].

Poly(3-hydroxybutyrate) (PHB) is one of the bacterially produced PHAs with high molecular weight. For the first time, PHB was isolated and characterised as long ago in 1925 by Lemoigne at the Pasteur Institute in Paris. PHB is produced as accumulated intracellular carbon source and energy reservoir by a variety of bacteria under a condition of nutrient deficiencies and an excess of carbon source [37]. A wide variety of microorganisms such as *Alcaligenes eutrophus* and *Pseudomonas oleovorans* accumulate PHB in the cell as energy and carbon storage products. The polymer itself proved to be a highly crystalline thermoplastic with a melting point around 180 °C.

PHB is often compared to polypropylene in its physical properties because they have similar melting point, degree of crystallinity and glass-transition temperature [36]. A recent new advanced transgenic technology has been employed to produce PHB in plants. The genes responsible for production of PHB extracted from bacteria are inserted into plant. As a result, PHB is produced in plant's leaves [38]. In Malaysia, PHB and PHBV have been extracted successfully by a research group in School of Biological Sciences, Universiti Sains Malaysia from palm oil in microorganisms of *Erwinia* [2,39].

The PHB's thermoplasticity, biocompatibility and biodegradability make it suitable for two applications: relieving environmental concerns caused by disposable of non-degradable plastics and providing new type of biomedical products. Moreover, some speciality applications of PHB have been reported as: firstly, PHB is optically active; each hydroxybutyrate monomer unit has a chiral carbon centre and every one of these is in the D (-) configuration (in alternative nomenclature this is the R form). Secondly, PHB is piezoelectric; the polymer molecules are arranged as 2/1 helices in orthorhombic crystals which does not have a centre of symmetry. Thus, if the crystals are deformed in a particular way the direction of average dipole moment will change and a polarisation will be produced.

Through applications of PHB, a wide number of deficiencies have prevented these applications. These are:

1. Bacterial PHB is stereoregular isotactic polyester and has high crystallinity of over 80% so that PHB exhibits great brittleness and poor impact resistance at room temperature
2. PHB is unstable in the molten state i.e. easily degrades.
3. Rate of degradation is not suitable for some application.

4. High production cost of PHB.

To overcome these drawbacks, PHB has been subjected to physical blending [4,16], biological modification [40] and materials loading (polymer-filler composites) [4].

The important factor and a real challenge of as mentioned drawbacks is thermal degradation of PHB. PHB undergoes intermolecular cis-elimination reaction. Scheme 1.3 represents the degradation of PHB where the elimination starts with the arrangement of PHB chains followed by breakage of C_α-C_β bonds.

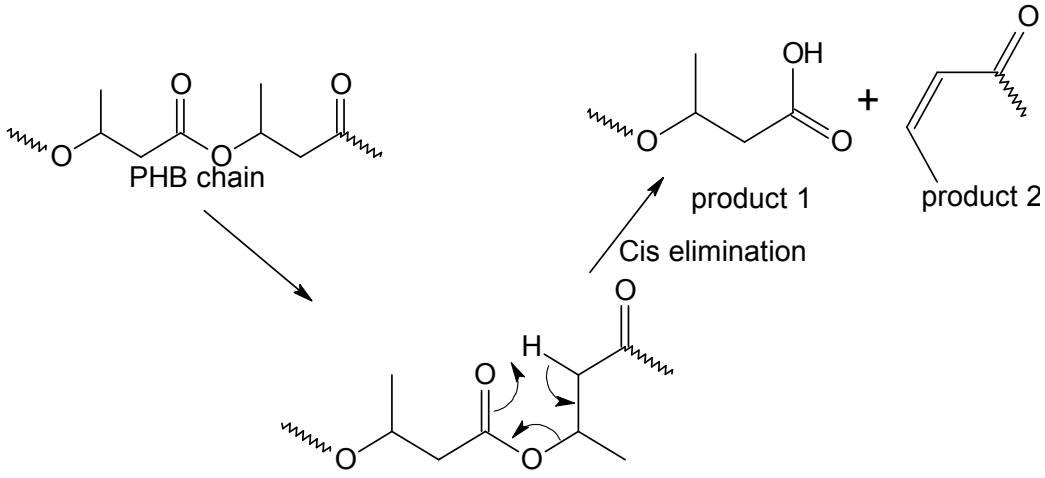

Scheme 1.3: PHB random chain scission [41].

1.5 Epoxidized Natural Rubber (ENR-50)

Natural rubber is cis-1,4-polyisoprene and the largest polymer component in tire [42]. Epoxidized Natural Rubber (ENR) is derived from the partial epoxidation of the natural rubber molecule, resulting in a totally new type of elastomer. The epoxide groups are randomly distributed along the natural rubber molecule. The double bonds of the isoprene unit are replaced with epoxide groups using in-situ performic acid epoxidation method. Scheme 1.4 shows the in situ performic acid epoxidation of NR.

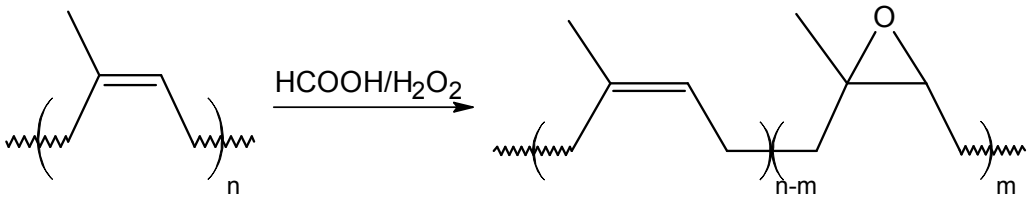

Scheme 1.4: In-situ performic acid epoxidation of natural rubber [43].

The levels of epoxide groups vary at approximately 10, 20, 30, 40, 50, 60 and 75 mole % epoxide affording ENR-10, ENR-20, ENR-30, ENR-40, ENR-50, ENR-60 and ENR-75, respectively.

Epoxidation results in a systematic increase in the polarity and glass transition temperature which can be reflected in various properties i.e. increase in damping, reduction in swelling in hydrocarbon oil, decrease in gas permeability, increase in silica reinforcement, improved compatibility with polar polymers like polyvinyl chloride, reduced rolling resistance and increased wet grip.

The excellent characteristic of ENR has also promoted its active involvement in rubber composition, polymer electrolytes, binders and reactive polymer blends. In tires industry, from 2007, a green product has been manufactured consisting of 97% non-petroleum based material in which ENR replaces the synthetic rubber as a major component. In the formulation of nanocomposites, ENR is used as a compatibilizer in the process of mechanical mixing [29,44,45].

ENR with 50% epoxidation (ENR-50) is the preferred polymer due to two promising properties; firstly, sufficient epoxide sites along entire length of polymer to avoid furanization and secondly high reactivity to ring opening reaction in

presence of nucleophile. The ring opening reaction of unsymmetrical epoxide like ENR under basic and acidic media can be described as in Scheme 1.5.

Conditon	Reaction
Acidic	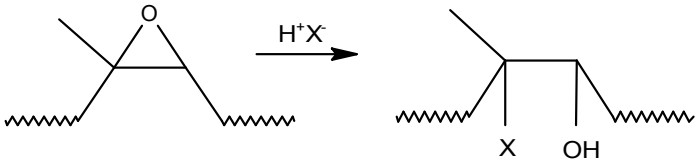
Basic	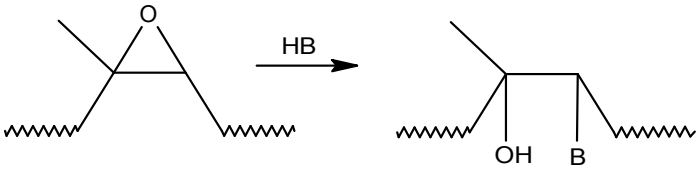

Scheme 1.5: Ring opening reaction of epoxide group of ENR chain under acidic and basic conditions [46].

1.6 PHB and ENR-based Immiscible Blends

The majority of the articles in the area of polymer blends focused on miscible polymer. In PHB-based immiscible blends with ethylene vinyl acetate (EVA) [47], epoxidized natural rubber (ENR) [2,16,17,48], thermoplastic starch (TPS) [37], ethylene propylene diene terpolymer (EPDM) [49], acrylonitrile-g-(ethylene-co-propylene-co-diene)-g-styrene [50] and poly(ε-caprolactone) (PCL) [13], polylactic acid (PLLA) [11], epichlorohydrin elastomers (PEP and ECO) [7] and polyethylene oxide (PEO) [51] have been reported.

In general, the polymer blends were prepared by two techniques, either solvent casting or mechanical mixing. The extent of the reaction is carried out as a factor of phase diffusion due to mechanical forces and heating. In an immiscible blending, the domain size affects the extent of miscibility by representing single T_g.

In fact, T_g depends on the strength of bonding and the level of reaction between domains.

The tensile properties and impact behavior of PHB/rubber have been reported by Abbate et al. [47]. They concluded a decrease in the particle size of the dispersed phase and an increased adhesion to the matrix yielded an improvement in the ultimate tensile properties, such as elongation at break and in the high-speed fracture toughness of these materials. Moreover, they mentioned the chemical interactions play an important role during the blending process. This was supported by morphological analysis that for PHB/EPR-g-succinic anhydride blend a graft copolymer is probably formed which can act as emulsifier and also compatibilizing agent between the PHB matrix and the un-reacted molecules of EPR-g-succinic anhydride.

The environmental degradation of PHB/lignin have been studied by Mousavioun et al. [52]. They reported that the thermal degradation of the buried PHB/lignin films follows a different degradation mechanism due to their weight loss profiles. The degradation mechanisms for PHB/lignin films are influenced by film composition and possible miscibility between the two components. XPS and FTIR showed that PHB in the blend undergoes hydrolytic degradation whilst buried in the soil whereas the lignin component remained intact. Lignin contains a variety of oxygen containing functional groups (e.g., hydroxyl and carboxylic acid) which could play a considerable role in antibacterial and antifungal activity.

The level of interaction, extent of miscibility and the morphology of a blend comprising PHB/PLLA have been published by Furukawa et al.[11]. They reported that the T_g values for PHB and PLLA components in the PHB/PLLA blends also do not change significantly. On the basis of T_c they suggested that each component in the

PHB/PLLA blends forms the mixed semicrystalline structures indicating that the PHB/PLLA blends with decreasing T_c are totally immiscible. They concluded that on the basis of micro IR spectrum from any spots of the PHB/PLLA (80/20) blends the crystalline bands are only due to PHB component and not the PLLA.

Lima and co-workers [7] have studied the phase behavior and morphology of PHB and epichlorohydrine elastomer blends, PEP/ECO. They deduced from the DSC and DMA results that PHB/PEP and PHB/ECO are both immiscible due to the melting temperature (T_m) of PHB in the blends where it decreases slightly with increasing elastomeric content and the melting point depression cannot be associated to miscibility, because the blends are immiscible. Therefore, T_m of the blends is affected by morphological effects. They mentioned there is an influence of PEP and ECO on the crystallization occurring upon cooling of PHB, even when the blends are immiscible due to an expressive decrease of the intensity of the peak at crystallization that is completed during the second heating. The degree of crystallinity of blends with PEP has been found to decrease with an increase in PEP content whereas PHB/ECO blends present degrees of crystallinity nearly independent of the ECO content.

The majority of research articles related to the ENR blend focuses on the compatibilizing properties [22,53], the activity [9,54] and the mechanical inducing properties [8,55] of ENR. Ismail and Hairunezam [53] examined the compatibilizer effect of ESBS on curing characteristics, mechanical properties and oil resistance of SBR/ENR blend and indicated that the increasing ENR content improves processability, tensile strength, tear strength and tensile modulus. In general the polymeric reaction is carried out during mixing where the chain diffuses from one phase to another phase. The crosslinking via radical reaction of poly(acrylic acid)

(PAA) [56], the reaction of hydroxyl and carbonyl groups of poly(ethylene-co-acrylic acid) (PEA) [57] and PMMA, respectively and crosslinking reaction [58] have been examined and the results published.

1.7 Clay

"Clay minerals" is in fact a term originally used by sedimentologists and soil scientists for the fraction of particles having very small size, with an equivalent diameter smaller than 2 μm, which is the clay fraction. Clay minerals consist mainly of hydrous layered magnesium or alumino-silicate and some geo-organic polymers are responsible for most surface and colloid reactions in the earth. In many of these minerals various metallic cations, such as lithium, magnesium and aluminum act as proxy wholly or in part for the magnesium, aluminum or silicon, respectively, with alkali metal and alkaline earth metal cations present as exchangeable cations. Each magnesium or alumino-silicate is composed of two types of sheets, octahedral and tetrahedral. The sheets are composed of planes of atoms, arranged one above the other, a plane of hydroxyls and/or oxygens above a plane of aluminium and/or magnesium or silicon. Scheme 1.6 indicates the classification of clay minerals according to the structure of silicate layers.

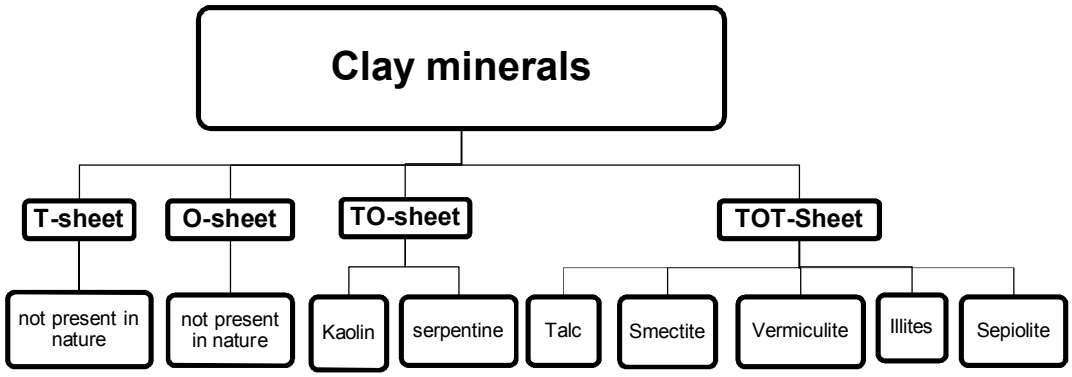

The terms T,O,TO and TOT represent tetrahedral, octahedral, a single tetrahedral sheet condensed with a single octahedral sheet and a central octahedral sheet sandwiched between two parallel tetrahedral sheets in one layer of clay minerals, respectively

Scheme 1.6: Clay minerals classifications [59].

In a tetrahedral sheet (T-sheet) a continuous linkage of SiO_4 tetrahedra through sharing of three O atoms with three adjacent tetrahedral produces a sheet with a planar network (Scheme 1.7a). The silica groups are arranged in the form of a hexagonal network with the final composition of $[Si_4O_{10}]^{4-}$.

An octahedral sheet (O-sheet) can be obtained through condensation of $Mg(OH)_6^{4-}$ or $Al(OH)_6^{4-}$ octahedral where each oxygen atom is shared by three octahedral but two octahedral can share only two neighboring O atoms giving rise a hexagonal network which is repeated indefinitely to form an $[Mg_6O_{12}]^{12-}$ or $[Al_4O_{12}]^{12-}$. Such a structure is shown in Scheme 1.7b.

A mineral layer of TO sheet of clay is composed of a single tetrahedral sheet condensed into a single octahedral sheet forming one unit layer. Here, the oxygens located at the apices of silica tetrahedral of the tetrahedral sheet and hydroxyls from one OH planes of octahedral sheet are condensed to form a single plane. The Si and Mg or Al atoms share 2/3 of oxygen atoms and protons and Mg or Al atoms share the remaining oxygen atoms. The ideal structural formulas of TO structure can be

suggested as $[(Mg/AL)_6\ Si_4O_{10}](OH)_8$. The view of TO-sheet is shown in Scheme 1.7c.

A layer of TOT-sheet is composed of one central octahedral sheet sandwiched between two parallel tetrahedral sheets. The majority type of clay in nature is of TOT structure. According to the structural formulas, TOT is divided into some sub-groups as talc-pyrophyllite, smectites, vermiculites and illites. The main differences between the subgroups are in the position of atoms and linkage between them. Smectite is the largest of the TOT family. It is sometimes called as montmorillonite group. A small fraction of tetrahedral Si atoms is substituted by Al/Mg fraction of octahedral atoms. The resulting charge deficiency is balanced by hydrated cations mainly K, Na, Ca and Mg. Smectites saturated with other cations dissociate in aqueous suspensions into exchangeable cations which are composed of several parallel TOT layers, held together by electrostatic forces by some of the exchangeable cations that remain in the interlayer space. Water and polar organic molecules can be attracted by the exchangeable cations and may intercalate. The interlayer space between TOT layers is obtained as a result of silicate layers expansion. The schematic representation of TOT clay and all subgroups are shown in Scheme 1.7d.

(a)	Tetrahedral sheet (T)	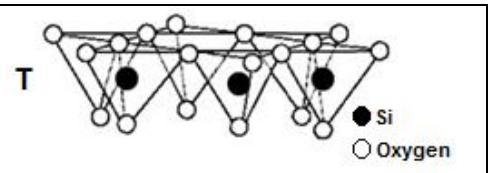
(b)	Octahedral sheet (O)	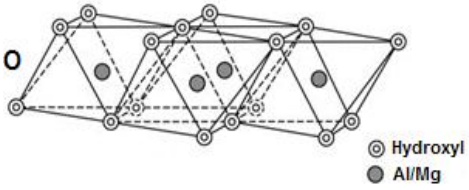
(c)	Tetrahedral-Octahedral sheet (TO)	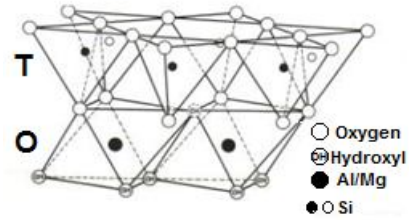
(d)	Tetrahedral-Octahedral-Tetrahedral sheet (TOT)	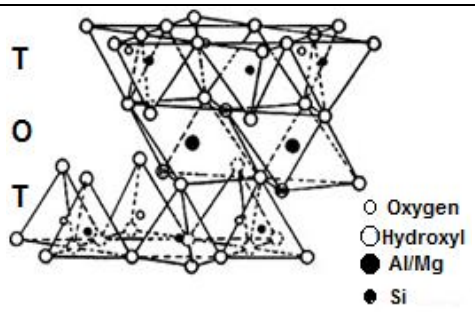

Scheme 1.7: The side view of various clay structures.

1.8 Swelling/Expansion of Silicate Layers in Montmorillonite

The clay of preference is montmorillonite (MMT) with micro/nano-sized particles formed by stacks of three-layer sandwiches: a layer of Mg or Al oxides in between the silicate layers. These sandwiches of 0.96 nm thickness and an average diameter of about 100 to 500 nm are the desired reinforcing entities for polymeric nanohybrids and nanocomposites. The chemical constitution of the MMT unit cell offers three types of reactive sites: anions on the silicate surface, hydroxyl (–OH)

groups and (few) cations on the narrow edges. The open structure of a montmorillonite is shown in Scheme 1.8. The basal spacing of such a structure takes a value between 1-2 nm.

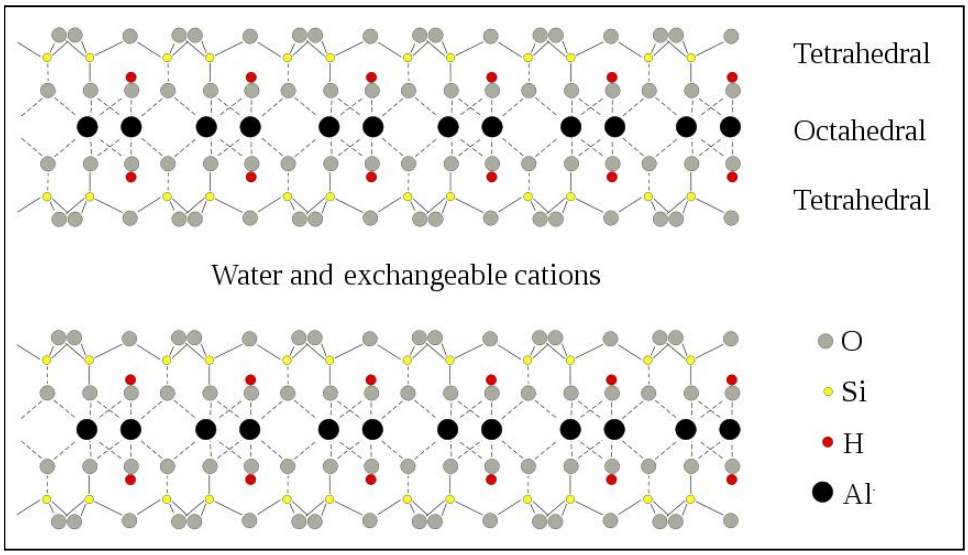

Scheme 1.8: Open structure of montmorillonite [60].

In general, compatibilisation/modification of clay is involved in forming an ionic bond between the clay surface and organophilic onium cations, especially alkyl ammonium. The advantage of this is that the chemical reaction not only changes the hydrophilic clay character into hydrophobic, but also it causes the clay particles to expand. The expansion means to intercalate as a first step to the total dispersion (exfoliation) of the clay. The disadvantage is that this chemical equilibrium process is diffusion controlled hence it may require an excess of intercalatant and it may take a long time to complete. An obvious sign of expansion behavior is increasing in basal spacing. Now a days, organomodification of clay, especially organomodified montmorillonite, have been manufactured by many factories like Nanocore (USA).

1.9 Organomodified Montmorillonite

The interactions between organic matter and clay minerals, either by cation exchange or adsorption of polar and nonpolar molecules is known as clay organomodification. The physical or chemical bonds are formed between the organic and inorganic matters. In majority of such a reaction, the clay minerals serve as the substrates and the organic entities are the adsorbed species. As a result of adsorption process, the properties of mineral clay may alter as follows:

1) The colloidal properties of the clay particles and the colloidal state of the system can change depending on the type of the organic compound and the ratio of inorganic/organic constituent [61].

2) The hydrophilicity of clay decreases as a result of replacement of inorganic cations by organic cations [59].

3) The activation energies of different reactions involving clay surfaces and organic compounds may either decrease or increase where clay substrates may serve as catalysts or inhibitors in different organic reactions [59,62,63].

4) The reactivity of adsorbed molecules between the silicate layers may differ by the hindrance and limitation effect of silicate layers into the orientation, motion and packing arrangement of the molecules [59].

The organomodification can occur either in nature or in laboratory. The source of natural organic matter is from biological matters and also from industrial and agrochemical man-made wastes.

The mechanism of adsorption of organic compounds inside the interlayer space of clay minerals has been reported with three types of organic matters namely organic cations, organic polar molecules and organic anions. The organic cationic species are generally reacted either by cation exchange or protonation of adsorbed

organic bases. For example, the exchange reaction between an inorganic clay metallic cation and an aqueous solution of an aliphatic ammonium salt can occur according to equation (1.5),

$$mR\text{-}NH_3Cl_{(aq)} + M^{m+}\text{—}Clay_{(Solid)} \longleftrightarrow MCl_{m(aq)} + (R\text{-}NH_3^{+})_m\text{—}Clay_{(Solid)} \quad (1.5)$$

The protonation occurs in various reaction levels namely surface hydrolysis of organic basic molecules, van der Waals interaction between the organic species and the oxygen planes and H-bonds between the organic species and basic sites. The adsorption of organic polar molecules is based on the Bronsted and Lewis theories on acids and bases accompanied by proton transfer from interlayer water to the organic molecules or formation of coordination bonds. The organic anions can interact by adsorption of negatively charged species only by formation of positively charged coordination species. The most important anionic organic matters are carboxylic acids by adsorption on the external broken-bonds surfaces.

1.10 Clay-Containing Polymeric Nanocomposites (CPNC)

For incorporation of clay into a polymeric matrix, the particles must be dispersed into individual stacks of platelets, and then delaminated into a uniform dispersion of individual platelets in the matrix. The process of delamination usually occurs through two stages: intercalation and exfoliation [61,62]. Some popular early texts in this area were published by Mortland [64], Utraki [65], Yariv and Cross [66] Pinnavaia and Beall [67], etc.

The clay of interest includes montmorillonite, hectorite, saponite, vermiculite, kaolinite, etc. The organic intercalant may be a cationic surface active agent generally a subgroup of alkyl ammonium salt like octadecyl trimethyl ammonium, dioctadecyl dimethyl, hexadecyl trimethyl, octadecyl amine, γ-aminopropyl triethoxysilane and many more. The polymeric matrix may be thermoplastic, thermoset and elastomeric.

Wang et al.,[68] have investigated the exfoliation process of magadiite in an epoxy matrix. They reported that depending on the kind of onium ions, intercalated or exfoliated nanocomposites can be obtained. They mentioned that a new type of exfoliated structure is also observed in which the nanolayer are regularly spaced over long distances (8 nm). The tensile properties of the polymer matrix were increased by the reinforcement effect of the silicate nanolayers.

Kaolinite, $Al_2Si_2O_5(OH)_4$, is a type of clay which has also received great interest in clay-based nanocomposites. The interactions of poly(acrylonitrile) (PAN) [69], poly(acryloamide) (PAA) [70] and poly(vinylpyrrolidone) (PVP) [71] have been realized.

Electroactive polymers intercalated in clays have been examined by several scientists. In this class of nanohybrids, the combination of clays and functional polymers interacting at atomic level [67]. In fact the ability of clays to interact with organic compounds exhibit relevant properties [72]. Clay may exhibit two opposite electrical properties related to their ionic conductivity. The insulating properties due to the presence of hydrated cations in the interlayer space and a significant conductivity of electrical signals associated with the ions from the clay interlayer region [73]. Here, there are two groups of conducting polymers: ion-conducting polymers like poly(ethylene oxide) (PEO) [74] and electronically conducting polymers

like polyacetylene (PA) [75], polyaniline (PANI) [76,77], polypyrrole (Ppy) [78,79] and polythiophene (PTh) [80].

Enhancements of polymer-layered silicate nanocomposite (PLSN) specially in mechanical properties [81], barrier [82–84], flammability resistance [85], oblation performance [86], environmental stability and solvent uptake [29,87] have been established.

The detailed structure-property of the nanoscale morphology of the layered silicate and the polymer is dominated by X-ray diffraction and transmission electron microscopy. Small-angle neutron scattering (SANS) may also be applied to determine d-spacing (d_{001}). This method is more sensitive and adaptable to different specimens, permitting the range of measurements to be extended to small angles. TEM may be used to determine the extent of intercalation/exfoliation. Conformation and crystallization behavior of the polymer matrix of CPNC have also been studied. The Si-O stretching vibration has been found to be very sensitive to long range interactions caused by expansion of interalayer spacing and/or imposed stress.

1.10.1 PHB/Clay Nanocomposites

A number of researchers have studied on PHB-based nanocomposites and nanohybrids motivated by strong desire to modify the physical and chemical properties of PHB by reducing the degree of crystallinity, modification of thermal behavior i.e. increasing or decreasing the thermal degradation, by controlling the spherulites size and improving the mechanical properties. The environmental concern became an important factor to production and syntheses of bio-based nanocomposites like PHB/clay. Most of the articles in this area were published from the year 2000 onwards.

PHB/clay nanocomposites have been successfully prepared by two procedures either by solution interaction [88–90] or mechanical mixing [41]. Among the precious clays that were used as filler, organically modified nanoclay have received great attention because of their potential to modify the properties of PHB. Thermal degradation is an important factor of PHB-based nanocomposites due to the significant instability of PHB at temperature close to the melting temperature. In general, the clay controls the thermal degradation due to the physical barrier [91], chain mobility, and the catalytic activity [89]. Moreover, the more hydrophobic the clay, the better dispersion in PHB as compare to the hydrophilic one [89,92]. The extent of interactions (intercalation or exfoliation) is another factor in thermal degradation [93]. Achilias and coworkers [94] reported that the intercalated structure can improve the thermal stability. The types of organic modifiers can also affect the thermal degradation. Surfactants like quaternary ammonium salts which is a common modifier enhance PHA degradation due to the catalytic properties of such materials [41]. The presence of Al-Lewis acid site and well-dispersed nanoclay are another factor which can control degradation [92]. Crystal size and degree of crystallinity in the case of PHB/clay restrict the mobility of polymer chain and caused reduction in thermal stability and melting temperature [95]. The barrier effect of silicate layers enhance the thermal stability of polymers by acting as thermal insulator and mass transport barrier during decomposition [96]. Changes in melting point are the result of many factors such as changes in molecular orientation, crystal thickness, and crystal perfection [97]. The change in onset temperature of decomposition can be attributed to the nanoscale of the MMT layers, preventing any out-diffusion of the volatile decomposition products [98]. It must be mentioned that the thermal degradation for the nanocomposites in the samples containing higher MMT content does not follow the

general trend due to the fact that the intercalated low molecular weight organic surfactant begins to lose, restricting of the thermal motion of polymer in the MMT interlayers and dispersion concept [98].

Many approaches have been developed to determine the kinetic parameters of PHB/MMT nanocomposites. The kinetic studies are motivated by the theories on the basis of graphical descriptions which are based on Arrhenius expression. Kissinger [93,99,100], Ozawa [99], Sestak-Berggren [94], Avrami-Erofeev [91,101,102] plots are the main theories in the determination of kinetic parameters.

The activation energy (E_a) of PHB in PHB/clay may decrease or increase upon increasing clay content. This trend is constant in most of the reported articles which is due to the surface interactions between the particles and the polymer matrix, providing an effective heat transfer between the particles and the polymer [100]. Hsu and coworkers [99] reported that E_a value of PHB/clay nanocomposites increased upon increasing clay content perhaps suggesting that the addition of clay caused more steric hindrance, decreasing the transportation ability of polymer chains, and then increasing the activation energy. The agglomeration of clay is a common phenomenon in non-linearity of E_a trends [96].

Crystallinity and degree of crystallinity is an important factor of crystalline polymers like PHB. The crystallization can be determined either by morphological studies based on spherulites size [89] or upon the thermal behavior of crystalline nanocomposites. The crystallization is governed by cooling rate and clay content in PHB/clay nanocomposites system [99]. By increasing the clay content, the crystallization rates become lower due to the limitation in transport ability of the polymer chains [99]. Clay particles act as strong nucleating agent for crystallization of polymer matrix [95,103]. It is reported that the mineral clay enhance the crystallization